

Observed sources and variability of Nordic seas overflow

Tor Eldevik^{1,2*}, Jan Even Ø. Nilsen^{1,2}, Doroteaciro Iovino^{1,2}, K. Anders Olsson^{2,3}, Anne Britt Sandø^{1,2} and Helge Drange^{1,2,4}

The overflows from the Nordic seas maintain the deep branch of the North Atlantic Ocean's thermohaline circulation^{1,2}, an important part of the global climate system^{3,4}. However, the source of these overflows, and of overflow variability, is debated: proposals include open-ocean convection, dense-water production on the Arctic shelves and the gradual transformation of Atlantic water as it circulates the periphery of the Nordic seas and the Arctic Ocean^{2,5,6}. Here we analyse time series of observed ocean temperature and salinity between 1950 and 2005. We find that the progression of thermohaline anomalies on interannual to decadal timescales does not support a systematic response of the overflow properties to convective mixing in the Greenland Sea as has been suggested^{7,8}. Instead, anomalies in temperature and salinity that leave the northern seas at the Denmark Strait have travelled along the rim of the Nordic seas from inflow to overflow. Furthermore, the Faroe–Shetland Channel reflects the variability of an overturning loop within the Norwegian Sea that has not been observed previously. We thus conclude that the Atlantic water circulating in the Nordic seas is the main source for change in the overflow waters.

The Atlantic Ocean is understood to be an important mediator of climate variability and change³. The main source of the southward flow of North Atlantic deep water is the overflow of dense water across the Greenland–Scotland ridge, which separates the Nordic seas from the Atlantic Ocean¹ (Fig. 1). The generation of overflow water is a matter of much debate. Proposed contributing processes and source regions are: open-ocean convection, primarily in the central Greenland Sea, dense water produced on the Arctic shelves and the gradual transformation of Atlantic water as it circulates the periphery of the Nordic seas and the Arctic Ocean^{2,5,6}. The state of the source regions can be related to the state of the overflows in two different ways: (1) prognostically through the degree of co-variability between the overflows and the sources upstream and (2) diagnostically through the decomposition of overflow into source waters. Observation-based descriptions so far have generally assessed the hydrography from individual cruises or climatology^{5,6}, and are thus concerned with diagnosis and the overflow composition of a steady state. The prognostic issues of variability, change and potential predictability⁹ remain unexplored in the long-term instrumental record.

Identifying the observed co-variability between overflows and sources—or the lack thereof—is the purpose of this study. To this end, a recently compiled comprehensive hydrographic database for the Nordic seas¹⁰ is used to construct time series of salinity and temperature for overflows and sources from 1950 to 2005 (Fig. 2).

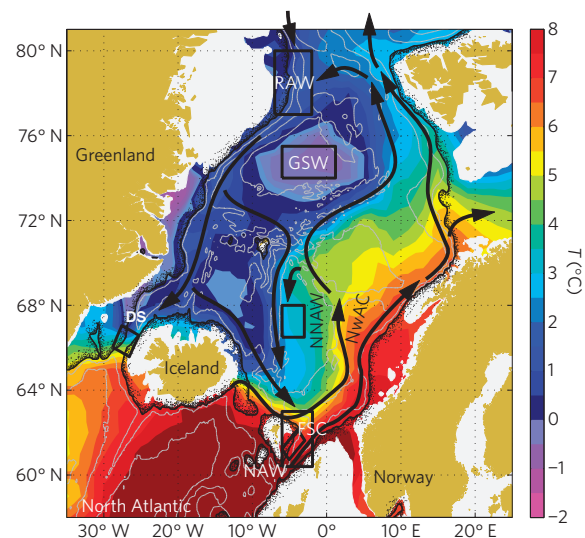


Figure 1 | Climatological temperature of the Nordic seas at 200 m depth.

The arrows indicate the pathways from warm and saline Atlantic inflow to dense overflow. Isobaths are given for every 1,000 m, and the thick 'pebbly' line at 500 m depth marks the continental slopes. Note the narrow gaps restricting the overflows.

Note that corresponding time series of volume fluxes cannot be constructed as current measurements are relatively few and limited to recent years^{11,12}. The regions and water masses extracted from the observations are restricted by the bounding boxes in Fig. 1 and further discussed in the Methods section. Greenland Sea water (GSW) represents the product of intermediate or deep open-ocean convection that fills the interior basins of the Nordic seas¹³, whereas return Atlantic water (RAW) is part of the more direct cyclonic loop from inflow of North Atlantic water (NAW) to dense overflow⁵. RAW is carried by the East Greenland current from the Fram Strait to the Denmark Strait, and the current entrains GSW en route⁶.

The above description is well established, but it has also been suggested that Denmark Strait overflow water (DS) is predominantly provided by a more eastern pathway rooted in the convective Iceland Sea¹⁴. This alternative mode of operation is not reflected in our database as time series specifically constructed for the Iceland Sea (not shown) were found to be less representative of overflow variability than what is described below for GSW, the main convective product in the Nordic seas. This alternative is therefore not further pursued herein.

¹G. C. Rieber Climate Institute, Nansen Environmental and Remote Sensing Center, Thormøhlensgate 47, N-5006 Bergen, Norway, ²Bjerknes Centre for Climate Research, Allégaten 55, N-5007 Bergen, Norway, ³Department of Chemistry, Göteborg University, SE-412 96 Göteborg, Sweden, ⁴Geophysical Institute, University of Bergen, Allégaten 70, N-5007 Bergen, Norway. *e-mail: tor.eldevik@nersc.no.

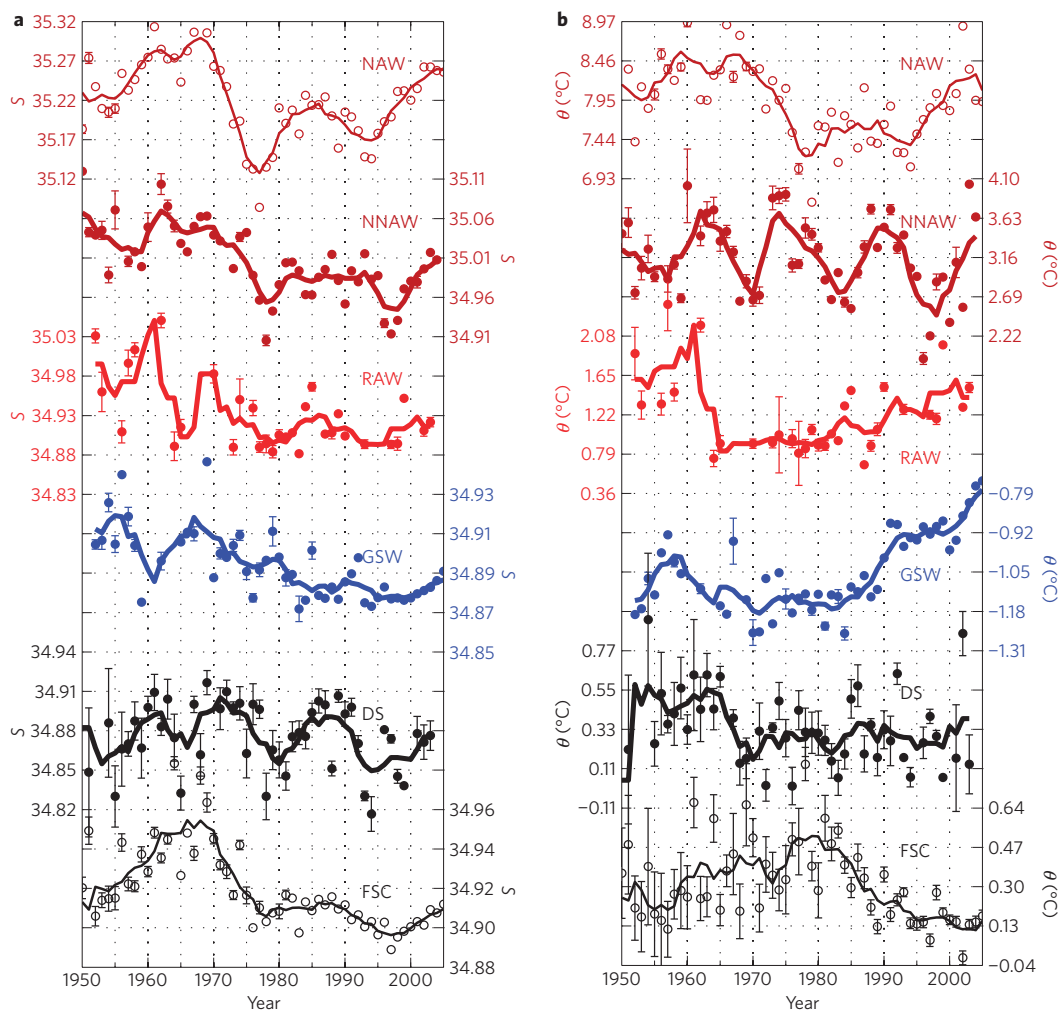


Figure 2 | The observational time series. a, Salinity S . **b**, Potential temperature θ . Water masses are labelled, data points are annual means and curves correspond to 5-year running means. Time series are normalized such that the vertical grid spacing is the standard deviation of the corresponding annual time series. Error bars show the error estimates of the annual means, $\sigma_m = \sigma / \sqrt{N-1}$, where σ is the standard deviation for the N observations within a year.

The overflow waters that do not leave through the Denmark Strait continue southeast to exit mainly through the Faroe–Shetland Channel along its western slope. Faroe–Shetland Channel overflow water (FSC) is also supported by the shorter pathway through the Jan Mayen Channel, which connects the Greenland Sea directly to the Norwegian Sea^{2,15}. There is also a shallow overflow between Iceland and the Faroe Islands, but this relatively weak outlet² is not considered herein.

An extra source for FSC can plausibly be found in the topographically steered retroflection from the western branch of the Norwegian Atlantic current¹⁶ (NwAC; Fig. 1). The resulting Norwegian North Atlantic water (NNAW) is sufficiently cold to have overflow density (Fig. 2), and it is a main water mass in the slope region north of the Faroe Islands¹⁷. This location, where the other two pathways to the Faroe–Shetland Channel also converge, is the entry point for the overflow water that constitutes FSC (ref. 18). Our inclusion of NNAW in the analysis provides a first quantification of this possible source.

The gradual transformation in Fig. 2—from warm and saline inflow to cold and relatively fresh overflow—is the result of the large oceanic heat loss and freshwater input in the Nordic seas and Arctic Ocean. All water masses show the regional freshening of the three decades before 1995 (ref. 19), but salinities increase notably thereafter, particularly for NAW (refs 12, 20). The freshening trend in the Denmark Strait is weak compared with the almost regular

decadal fluctuations there. The ‘great salinity anomaly’²¹ is seen in RAW and DS around 1965, and in NAW, NNAW, RAW and DS in the second half of the 1970s. The interannual to decadal variability is also broadly reflected in the observed temperatures, but cooling trends corresponding to the long-term freshening are generally less distinct or absent. GSW exhibits a strong warming after 1980, whereas the overflows do not.

With this unique collection of observational time series at hand, it is possible to quantify objectively to what extent the overflows manifest the thermohaline variability of the sources upstream. We do this by cross-correlations, a simple and common way to assess the possible progression of anomalies through a collection of time series. The lagged peak correlations between the detrended versions of the annual time series in Fig. 2 are given in Table 1. We emphasize that the analysis includes the most commonly suggested sources for overflow in the Nordic seas^{2,5,22}. One would therefore expect overflow variability that is not accounted for by Table 1 to be partly stochastic. Extra variability due to, for example, other sources or nonlinear relations, is not considered herein. The latter is however represented to the extent that it contributes to variable overflow compositions as diagnosed in Fig. 4.

Starting with the Denmark Strait, the main overflow from the Nordic seas, we find no significant correlation with GSW for potential temperature, and there is only a weak negative correlation for salinity. A signature of the water mass transformation taking

Table 1 | Lagged peak correlations.

	NAW	NNAW	RAW	GSW
Salinity				
NNAW	0.60@1 yr	—	—	—
RAW	0.49@1 yr	0.37@0 yr	—	—
GSW	÷	0.30@-2 yr	-0.34@1 yr	—
DS	0.37@2 yr	÷	0.46@1 yr	-0.28@1 yr
FSC	0.61@0 yr	0.50@1 yr	÷	0.42@0 yr
Temperature				
NNAW	÷	—	—	—
RAW	0.47@1 yr	-0.43@3 yr	—	—
GSW	÷	÷	0.62@0 yr	—
DS	÷	0.30@-1 yr	0.42@2 yr	÷
FSC	-0.38@-1 yr	0.33@3 yr	-0.54@0 yr	-0.60@-1 yr

Time lags are given relative to the water masses in the top row. All tabulated correlations (*r*) were calculated using detrended annual time series and are significant above the 90% confidence level using the *t*-test $t = r / \sqrt{(1-r^2)/(N-2)}$, where *N* is the degrees of freedom when auto-correlation has been accounted for; '÷' indicates no such correlation. The relations in bold are those shown in Fig. 3.

place directly in the flow of Atlantic-derived waters is more distinct. The sequence of events suggested by Table 1 is illustrated in Fig. 3a, b: the variability of the inflow (NAW) is reflected both in salinity and temperature in the Fram Strait (RAW), and variability in RAW and NAW is subsequently reflected in DS. The dissimilarities between NAW and RAW time series around the second half of the 1960s can be explained by the onset of the great salinity anomaly²¹ and the strong heat loss associated with the anomalous cold winters of the period¹³.

The time lags in Table 1 are only approximations of the travel times of actual thermohaline anomalies as the time series are auto-correlated to a varying degree (integral timescales ranging from <1 to 3.5 years) and because of the above-mentioned stochasticity. Slight differences in time lags between salinity and temperature can therefore be expected, and similarly, partial lags may not exactly add up to the time lag between two end points estimated directly. The lags involved in Fig. 3a, b are nevertheless roughly in agreement with other studies: a two-year transit time south from the Fram Strait to both overflows can be estimated from a recent tracer release experiment^{15,23}, and anomalies in the inflow have been observed to reach the Fram Strait with NwAC in 1–3 years^{20,24}. The short NAW–RAW time lag is thus related to the circulation within the Nordic seas, and not to the extended pathways through the Arctic Ocean. This does not exclude a role for water mass transformation in the Arctic proper⁶, as the associated variability is captured only to the extent that it is included in RAW (see the Methods section).

Moving to the Faroe–Shetland Channel, salinity provides the single case where overflow variability resembles that of GSW. The highest FSC correlation is however with NAW salinity at no lag (Table 1). This is indicative of a direct influence of the inflow on the overflow below, or, keeping auto-correlation in mind, an overturning loop local to the southern Norwegian Sea (there is also a second peak correlation of 0.56 at 2 year lag). Separate and stronger evidence in favour of our suggested NAW–NNAW–FSC loop is provided by the fact that anomalies progress from NAW to the recirculating NNAW, and then from NNAW back to FSC (both lagged by 1 year; see Fig. 3c).

There is also a positive NNAW–FSC correlation in temperature, but a progression of thermal anomalies is not obvious from a visual inspection of Fig. 2b. The most notable co-variability is how FSC tends to cool when RAW or GSW warms. Temperature

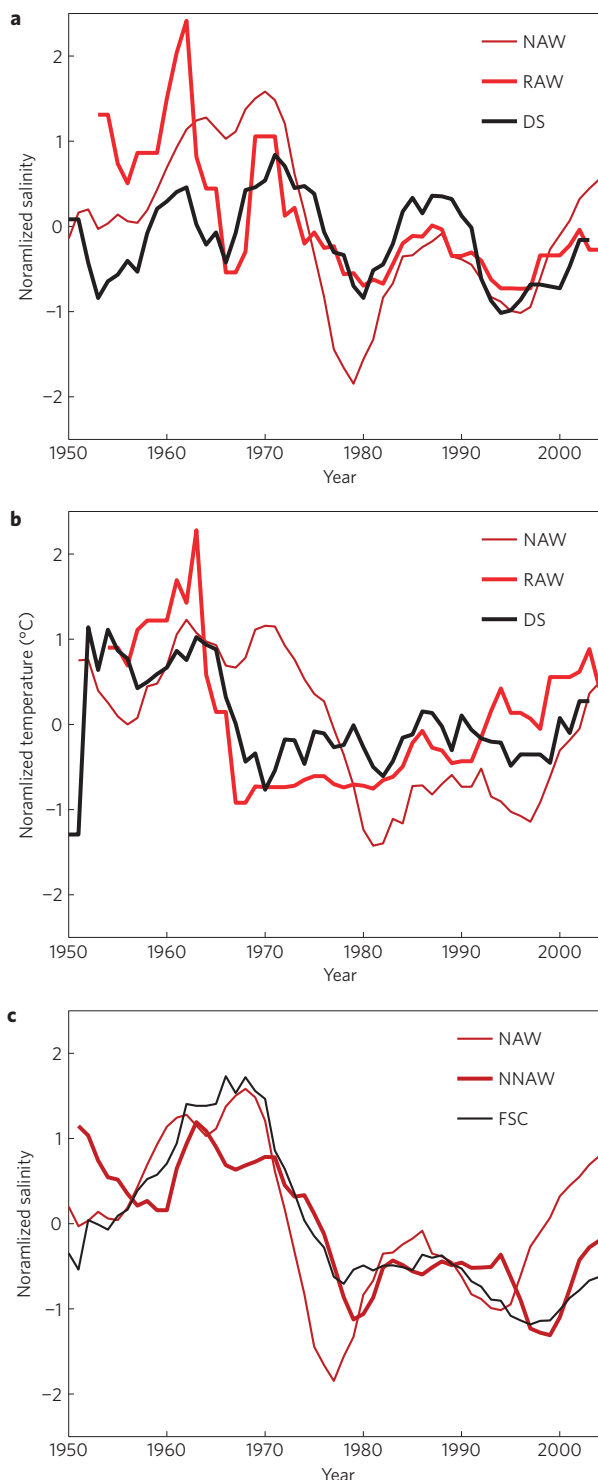


Figure 3 | Normalized time series of overflow hydrography and Atlantic-derived sources of variability. a, DS salinity. b, DS temperature. c, FSC salinity. Curves are as in Fig. 2, and the sources shifted to the right using the time lags in bold in Table 1.

anomalies in FSC must therefore relate more to a changing partition of warm versus cold source waters in the overflow²⁵, than to the export of anomalies from an individual source upstream. It is a common finding in idealized model studies that the relative importance of pathways, and thus overflow composition, is sensitive to interannual changes in the large-scale winds that force the barotropic circulation in the Nordic seas^{26,27}.

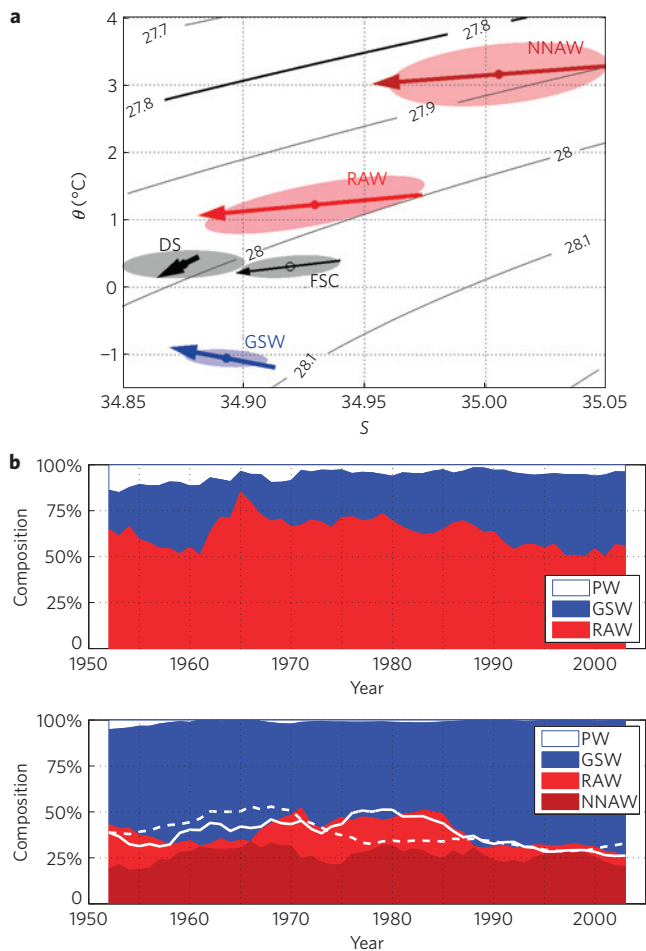


Figure 4 | Thermohaline properties of sources and overflows, and the associated overflow compositions. **a**, Arrows show linear trends for the full time period, and variance ellipses show water mass variability around mean properties. Contour lines are isopycnals. **b**, The overflow decompositions (DS, top; FSC, bottom) were done as described in the main text using the smoothed time series in Fig. 2 at no lag. The FSC composition is overlaid by appropriately scaled FSC temperature (solid line) and salinity (dashed line) at the interface between warm and saline (NNAW, RAW), and cold and fresh (GSW, PW) water masses.

The mean properties and variability of sources and overflows are summarized in the θ - S diagram of Fig. 4a. The offset of DS from the RAW-GSW mixing line is consistent with a slight addition of polar water⁶ (PW; $S = 34.2$, $\theta = -1.6$ °C, assumed constant). The mean mixture producing DS is 5% PW, 31% GSW—representing the Nordic seas' convective basins in general—and 64% RAW. Assuming that Denmark Strait hydrography also applies slightly upstream where the East Greenland current branches off, the three pathways previously described to feed FSC can be represented by DS, GSW and NNAW, respectively (see Fig. 1). FSC is consistently situated within the 'thermohaline triangle' spanned out by NNAW, GSW and DS in Fig. 4a, corresponding to a mean FSC composition of 1% PW, 61% GSW, 12% RAW and 26% NNAW.

The Denmark Strait overflow volume transport is about 3/2 that of the Faroe-Shetland Channel². More than 50% of the combined overflow is thus associated with the circulation of Atlantic-derived waters, and about 40% is associated with the GSW-like water masses characteristic of the Nordic seas' interior. These simple estimates of overflow composition are in qualitative agreement with more detailed assessments^{23,28}. The assumed compositions' evolution in time are shown in Fig. 4b. Note how the varying partition between

warm and saline, and cold and fresh sources of FSC more reflects temperature than salinity as suggested above.

Figure 4a offers a simple explanation of the observed variability: fluctuations in water mass salinities are as large as the salinity contrast between sources, and particularly so for NNAW and RAW. The situation is the opposite for potential temperature where the contrast between water masses dominates over the individual variability. The θ - S diagram, in consistency with Figs 3, 4b, thus suggests two basic mechanisms for overflow variability in the present climate: overflow salinities reflect the variable salinity of individual sources, whereas overflow temperatures are more likely to reflect a variable overflow composition as is the case for FSC.

Our study constitutes a first observation-based synthesis of the thermohaline variability of overflows and sources on interannual to decadal timescales. The long observational time series presented provide a qualitative and quantitative benchmark against which both numerical models and conceptual descriptions of the Atlantic Ocean/Nordic seas thermohaline circulation can be tested. A coherent variability in the overflows relating to convective mixing in the Greenland Sea—a common finding in many of the present climate models^{8,29}—is for example not evident from the available observations. Possible predictability⁹ would seem more related to the Nordic seas' circulation of Atlantic-derived waters as it contributes to most variability involving the overflows herein.

Methods

The boxes in Fig. 1 are the water columns used to deduce water masses from the observations using the following criteria: NNAW is the average salinity and temperature between 75 and 350 m, representative of the Atlantic-derived salinity maximum; RAW is the average salinity and temperature properties between 240 and 450 m, the depth range where the Atlantic signature of maximum salinity and temperature is found; GSW is defined as the homogeneous water between 550 and 950 m depth; overflows DS and FSC are defined using the common definition^{1,2} $\sigma_\theta > 27.8$ (potential temperature is restricted to $\theta < 3$ °C in the Denmark Strait to exclude the occasional influence of inflowing Atlantic waters); and NAW is simply defined as 'non-overflow' water ($\sigma_\theta \leq 27.8$). The NAW box extends slightly into the Norwegian Sea so that it includes the Faroe current from the west, thus accounting for both branches of Atlantic inflow that form the NwAC.

The common water mass RAW is used to characterize the southward flow of Atlantic-derived waters with the East Greenland current. The water mass represents the two varieties of Atlantic waters in the Fram Strait, the recirculation within the Nordic seas and the colder counterpart that has travelled the Arctic Ocean. Unfortunately, the two cannot systematically be distinguished to make separate time series in our database. This difficulty also seems to apply to individual profiles and sections from dedicated oceanographic surveys³⁰, and as a result the two are often considered one common water mass in the East Greenland current^{13,30}, consistent with our approach.

In a recent review of the Denmark Strait overflow²², a distinction is made between overflow water in general ($\sigma_\theta > 27.8$), and a more conservative threshold ($\sigma_\theta > 27.85$) characteristic of the dense-water plume that descends the continental slope into the deep North Atlantic Ocean. DS time series are insensitive to this distinction (allowing for a slight shift in mean properties) as the defining box largely excludes the Greenland shelf region (see Fig. 1) where the overflow water that is not part of the plume is found²².

In general, and even if the names given to the water masses may differ in detail from those found elsewhere, the different water masses presented herein (Figs 2 and 4a) are in good agreement with the observational literature, both that specific to regions or water masses^{11,17,22,30}, and the more overview descriptions of the Nordic seas and the overflows^{2,6,13}.

Received 1 December 2008; accepted 9 April 2009;
published online 3 May 2009

References

- Dickson, R. R. & Brown, J. The production of North Atlantic deep water: Sources, rates and pathways. *J. Geophys. Res.* **99**, 12319–12342 (1994).
- Hansen, B. & Østerhus, S. North Atlantic–Nordic Seas exchanges. *Prog. Oceanogr.* **45**, 109–208 (2000).
- Rahmstorf, S. Ocean circulation and climate during the past 120,000 years. *Nature* **419**, 207–214 (2002).
- Kleiven, H. F. *et al.* Reduced North Atlantic deep water coeval with the glacial Lake Agassiz fresh water outburst. *Science* **319**, 60–64 (2008).

5. Mauritzen, C. Production of dense overflow waters feeding the North Atlantic across the Greenland–Scotland Ridge. Part 1: Evidence for a revised circulation scheme. *Deep-Sea Res. I* **43**, 769–806 (1996).
6. Rudels, B., Friedrich, H. J. & Quadfasel, D. The arctic circumpolar boundary current. *Deep-Sea Res. II* **46**, 1023–1062 (1999).
7. Schlosser, P., Bönisch, G., Rhein, M. & Bayer, R. Reduction of deepwater formation in the Greenland Sea during the 1980s: Evidence from tracer data. *Science* **251**, 1054–1056 (1991).
8. Dong, B. & Sutton, R. W. Mechanism of interdecadal thermohaline circulation variability in a coupled ocean–atmosphere GCM. *J. Clim.* **18**, 1117–1135 (2005).
9. Dickson, B., Meincke, J., Vassie, I., Jungclaus, J. & Østerhus, S. Possible predictability in overflow from the Denmark Strait. *Nature* **397**, 243–246 (1999).
10. Nilsen, J. E. Ø., Hátún, H., Mork, K. A. & Valdimarsson, H. *The NISE Data Set*. Technical Report 08-01 (Faroese Fisheries Laboratory, Box 3051, Tórshavn, Faroe Islands, 2008).
11. Hansen, B. & Østerhus, S. Faroe Bank Channel overflow 1995–2005. *Prog. Oceanogr.* **75**, 817–856 (2007).
12. Skagseth, Ø. *et al.* in *Arctic–Subarctic Ocean Fluxes: Defining the Role of the Northern Seas in Climate* (eds Dickson, B., Meincke, J. & Rhines, P.) 45–64 (Springer, 2008).
13. Blindheim, J. & Østerhus, S. in *The Nordic Seas: An Integrated Perspective* (eds Drange, H., Dokken, T. M., Furevik, T., Gerdes, R. & Berger, W.) 11–38 (Geophysical Monograph Series 158, American Geophysical Union, 2005).
14. Jonsson, S. & Valdimarsson, H. A new path for the Denmark Strait overflow water from the Iceland Sea to Denmark Strait. *Geophys. Res. Lett.* **31**, L03305 (2004).
15. Olsson, K. A. *et al.* Intermediate water from the Greenland Sea in the Faroe Bank Channel: Spreading of released sulphur hexafluoride. *Deep-Sea Res. I* **52**, 279–294 (2005).
16. Poulain, P.-M., Warn-Varnas, A. & Niiler, P. P. Near-surface circulation of the Nordic seas as measured by Lagrangian drifters. *J. Geophys. Res.* **101**, 18237–18258 (1996).
17. Read, J. F. & Pollard, R. T. Water masses in the region of the Iceland–Færoes front. *J. Phys. Oceanogr.* **22**, 1365–1378 (1992).
18. Søiland, H., Prater, M. D. & Rossby, T. Rigid topographic control of currents in the Nordic Seas. *Geophys. Res. Lett.* **35**, L18607 (2008).
19. Curry, R. & Mauritzen, C. Dilution of the northern North Atlantic Ocean in recent decades. *Science* **308**, 1772–1774 (2005).
20. Holliday, N. P. *et al.* Reversal of the 1960s to 1990s freshening trend in the northeast North Atlantic and Nordic Seas. *Geophys. Res. Lett.* **35**, L03614 (2008).
21. Dickson, R. R., Meincke, J., Malmberg, S.-A. & Lee, A. J. The great salinity anomaly in the Northern North Atlantic 1968–1982. *Prog. Oceanogr.* **20**, 103–151 (1988).
22. Dickson, B. *et al.* in *Arctic–Subarctic Ocean Fluxes: Defining the Role of the Northern Seas in Climate* (eds Dickson, B., Meincke, J. & Rhines, P.) 443–474 (Springer, 2008).
23. Olsson, K. A., Jeansson, E., Tanhua, T. & Gascard, J.-C. The East Greenland current studied with CFCs and released sulphur hexafluoride. *J. Mar. Syst.* **55**, 77–95 (2005).
24. Furevik, T. On anomalous sea surface temperatures in the Nordic Seas. *J. Clim.* **13**, 1044–1053 (2000).
25. Turrell, W. R., Slesser, G., Adams, R. D., Payne, R. & Gillibrand, P. A. Decadal variability in the composition of Faroe–Shetland Channel bottom water. *Deep-Sea Res. I* **46**, 1–25 (1999).
26. Eldevik, T., Straneo, F., Sandø, A. B. & Furevik, T. in *The Nordic Seas: An Integrated Perspective* (eds Drange, H., Dokken, T. M., Furevik, T., Gerdes, R. & Berger, W.) 89–104 (Geophysical Monograph Series 158, American Geophysical Union, 2005).
27. Käse, R. H., Serra, N., Köhl, A. & Stammer, D. Mechanisms for the variability of dense water pathways in the Nordic Seas. *J. Geophys. Res.* **114**, C01013 (2009).
28. Mauritzen, C. Production of dense overflow waters feeding the North Atlantic across the Greenland–Scotland Ridge. Part 2: An inverse model. *Deep-Sea Res. I* **43**, 807–835 (1996).
29. Guemas, V. & Salas-Méla, D. Simulation of the Atlantic Meridional Overturning Circulation in an Atmosphere–Ocean Global Coupled Model. Part I: A mechanism governing the variability of ocean convection in a preindustrial experiment. *Clim. Dyn.* **31**, 29–48 (2007).
30. Rudels, B. *et al.* The interaction between waters from the Arctic Ocean and the Nordic Seas north of Fram Strait and along the East Greenland current: Results from the Arctic Ocean-02 Oden expedition. *J. Mar. Syst.* **55**, 1–30 (2005).

Acknowledgements

This research was supported by the Norwegian Research Council through the projects ProClim, POCAHONTAS, BIAC and NorClim. The data were provided by the Marine Research Institute, Iceland; Institute of Marine Research, Norway; the Faroese Fisheries Laboratory; Geophysical Institute, University of Bergen, Norway; and the Arctic and Antarctic Research Institute, Russia, through the NISE project. The authors are grateful for discussions with numerous colleagues, particularly P. E. Isachsen, J. Lilly, K. Lygre, K. Oliver, Ø. Skagseth and D. J. Steinskog. This is publication No. A225 from the Bjerknes Centre for Climate Research.

Additional information

Reprints and permissions information is available online at <http://npg.nature.com/reprintsandpermissions>. Correspondence and requests for materials should be addressed to T.E.